MATCH
Communications in Mathematical and in Computer Chemistry

MATCH Commun. Math. Comput. Chem. **92** (2024) 437–482
ISSN: 0340–6253
doi: 10.46793/match.92-2.437L

Dynamic Exploration and Control of Bifurcation in a Fractional–Order Lengyel–Epstein Model Owing Time Delay

Peiluan Li[a,b], **Yuejing Lu**[a,b], **Changjin Xu**[c,*], **Jing Ren**[a,b]

[a] *School of Mathematics and Statistics, Henan University of Science and Technology, Luoyang 471023, PR China*

[b] *Longmen Laboratory, Luoyang, Henan, 471003, PR China*

[c] *Guizhou Key Laboratory of Economics System Simulation, Guizhou University of Finance and Economics, Guiyang 550025, PR China*

9902639@haust.edu.cn, 220320080782@stu.haust.edu.cn, xcj403@126.com, 220320080769@stu.haust.edu.cn

(Received November 11, 2023)

Abstract

Delayed differential equation plays a vital role in revealing the dynamics of chemical reaction law. In this work, we propose a novel fractional-order Lengyel-Epstein model owing time delay. By regarding the delay as parameter and investigating the distribution of roots of the associated characteristic equation of the formulated fractional-order delayed Lengyel-Epstein model, we set up a new delay-dependent criterion on stability and bifurcation of the involved fractional-order delayed Lengyel-Epstein model. Making use of nonlinear delayed feedback controller, we can effectually control the stability domain and the time of bifurcation phenomenon of the formulated fractional-order delayed Lengyel-Epstein model. Taking advantage of hybrid controller, we are able to adjust the stability domain and the time of bifurcation phenomenon of the established fractional-order delayed Lengyel-Epstein model. The study shows that delay is a vital factor which affects the stability and bifurcation behavior of the addressed fractional-order delayed Lengyel-Epstein

*Corresponding author.

model. In order to illustrate the rationality of the acquired theoretical outcomes, we execute Matlab simulations to check this fact. The gained outcomes in this work are absolutely innovative and possess enormous theoretical significance in adjusting concentrations of different chemical substance.

1 Introduction

Nowadays delayed differential equation has been widely considered to be a very important tool to give a description of practical chemical reaction. Through the construction of chemical reaction model by using delay differential equation, we can effectively reveal the inherent law of different chemical reaction substances. During the past decades, a great deal of scholars pay great attention to dynamical behavior of various chemical reaction systems and lots of valuable fruits on many chemical reaction dynamical models have been reported. For example, Din et al. [1] explored the stability, Hopf bifurcation and control of chaos for a chlorine dioxide-iodine-malonic acid reaction model; Sekerci and Petrovskii [2] dealt with the dynamical behavior of a plankton-oxygen models under the the changing climate conditions; In 2022, Mondal and Samanta [3] discussed the stability and bifurcation phenomenon of a delayed toxin producing plankton model owing time delays and variable search rate of zooplankton; In the work of Gökçe et al. [4], the authors investigated the Hopf bifurcation and stability of spatial patterns of a diffusive oxygen–plankton system concerning delays; In 2015, Xu and Wu [5] carried out a detailed analysis on Hopf bifurcation and chaos control for a chemical reaction model; Wang and Jia [6] focused on stability and Hopf bifurcation in a Gray-Scott chemical reaction system. For more related contents, one can see [7–12].

In 1991 and 1992, Lengyel and Epstein [13, 14] established the following chemical reaction model(i.e., Lengyel-Epstein model) to describe the

reaction process of two chemical reactants:

$$\begin{cases} \dfrac{\partial x_1}{\partial t} = \triangle x_1 + \alpha - x_1 - \dfrac{4x_1x_2}{1+x_1^2}, t > 0, y \in \Omega, \\ \dfrac{\partial x_2}{\partial t} = \gamma \left[c\triangle x_2 + \beta \left(x_1 - \dfrac{x_1x_2}{1+x_1^2} \right) \right], t > 0, y \in \Omega, \\ \dfrac{\partial x_1}{\partial n} = \dfrac{\partial x_2}{\partial n} = 0, t > 0, y \in \partial\Omega, \\ x_1(y,0) = x_{1_0}(y) \geq 0, x_2(y,0) = x_{2_0}(y) \geq 0, y \in \Omega, \end{cases} \tag{1}$$

where $x_1(y,t)$ and $x_2(y,t)$ stand for the concentrations of both chemical reactants, respectively, $\alpha > 0$ and $\beta > 0$ are real constants that represent the quantities affiliated with the feed concentrations, c and $\gamma > 0$ stand for the ratio of diffusion coefficients and the rescaling parameter, respectively; Ω denotes a bounded open domain in R with smooth boundary $\partial\Omega$, and $\triangle$ dentes the Laplace operator. In details, one can see [13,14]. Model (1) has been widely investigated by numerous researchers. Yi et al. [15] studied the global asymptotical stability of model (1); Yi et al. [16] handled the diffusion-driven instability and Hopf bifurcation of model (1); Ni and Tang [17] discussed the Turing patterns of model (1); Jin et al. [18] analyzed the bifurcation issue of patterned solutions of model (1).

As we know that the development of things depends on both current time and past history. Thus in many cases, delay often exist in ordinary differential systems. If we ignore the delay, then some errors will occur. Generally speaking, delay will result in the loss of stability of system. Based on this viewpoint, Celik et al. [19] set up the following delayed Lengyel-Epstein model:

$$\begin{cases} \dfrac{dx_1(t)}{dt} = \alpha - x_1(t) - \dfrac{4x_1(t)x_2(t-\theta)}{1+x_1^2(t)}, \\ \dfrac{dx_2(t)}{dt} = \gamma\beta \left[x_1(t) - \dfrac{x_1(t)x_2(t-\theta)}{1+x_1^2(t)} \right], \end{cases} \tag{2}$$

where θ stands for a delay. Applying the stability and bifurcation theory of integer-order delayed differential equation, Çelik and Merdan [19] explored the Hopf bifurcation problem of system (2). In 2015 and 2016, Merdan and Kayan [20,21] proposed and carried out the Hopf bifurcation analysis

of the following two delayed Lengyel-Epstein models:

$$\begin{cases} \dfrac{dx_1(t)}{dt} = \alpha - x_1(t) - \dfrac{4x_1(t-\theta)x_2(t)}{1+x_1^2(t)}, \\ \dfrac{dx_2(t)}{dt} = \gamma\beta\left[x_1(t) - \dfrac{x_1(t-\theta)x_2(t)}{1+x_1^2(t)}\right], \end{cases} \tag{3}$$

and

$$\begin{cases} \dfrac{dx_1(t)}{dt} = \alpha - x_1(t-\theta) - \dfrac{4x_1(t-\theta)x_2(t)}{1+x_1^2(t)}, \\ \dfrac{dx_2(t)}{dt} = \gamma\beta\left[x_1(t-\theta) - \dfrac{x_1(t-\theta)x_2(t)}{1+x_1^2(t)}\right]. \end{cases} \tag{4}$$

In 2020, Zhang and He [22] proposed the following delayed Lengyel-Epstein model:

$$\begin{cases} \dfrac{dx_1(t)}{dt} = \alpha - x_1(t-\theta) - \dfrac{4x_1(t)x_2(t)}{1+x_1^2(t)}, \\ \dfrac{dx_2(t)}{dt} = \gamma\beta\left[x_1(t) - \dfrac{x_1(t)x_2(t)}{1+x_1^2(t)}\right]. \end{cases} \tag{5}$$

By choosing the delay as parameter, Zhang and He explored the multiple stability switches and delay-induced Hopf bifurcations of system (5).

Considering that there are different feedback delays in the development of the concentrations of both chemical reactants, Li and Zhang [23] built the following delayed Lengyel-Epstein model:

$$\begin{cases} \dfrac{dx_1(t)}{dt} = \alpha - x_1(t-\theta_1) - \dfrac{4x_1(t-\theta_1)x_2(t-\theta_2)}{1+x_1^2(t-\theta_1)}, \\ \dfrac{dx_2(t)}{dt} = \gamma\beta\left[x_1(t-\theta_2) - \dfrac{x_1(t-\theta_2)x_2(t-\theta_1)}{1+x_1^2(t-\theta_2)}\right], \end{cases} \tag{6}$$

where θ_1 and θ_2 stand for two different delays.

It is worth mentioning that all the considered works above on Lengyel-Epstein model (see [1–22]) only focus on the integer-order chemical reaction models. Recently, a great deal of works show that fractional-order dynamical equation can be thought as a more effective tool to portray the real natural law in the natural world than the classical integer-order counterparts. The suty shows that fractional dynamical equation has been widely applied numerous fields such as neural networks, financial engineering, artificial intelligence, various physical waves, elastic mechanics,

capacitor principle, biomedical technique, automation, cryptology and so on [24–29]. All these applications are derived from the great memory peculiarity and hereditary function for all kinds of materials and change process [30, 31]. At the present time, fractional-order dynamical models have aroused much interest from lots of scholar and enormous accomplishments have been gained. For example, Lin et al. [32] carried out the output synchronization exploration and PD control issue of coupled fractional delayed neural networks; Popa [33] explored the Mittag–Leffler stability behavior and synchronization problem of neutral-type fractional neural networks owing mixed delays and leakage delay; Yousef et al. [34] revealed the impact of fear for a fractional prey-predator model owing predator density-dependent prey mortality; Rihan and Rajivganthi [35] dealt with the stability and bifurcation of a fractional-order delayed predator-prey model concerning Holling-type III function. For more related works, one can see [36–40].

Noticing that the fractional-order delayed Lengyel-Epstein model can better reflect the memory trait and hereditary superiority of the concentrations of both chemical reactants and stimulated by the analysis above and relying on model (6), in this article, we are going to build the following fractional-order delayed Lengyel-Epstein model:

$$\begin{cases} \dfrac{d^{\rho}x_1(t)}{dt^{\rho}} = \alpha - x_1(t-\theta_1) - \dfrac{4x_1(t-\theta_1)x_2(t-\theta_2)}{1+x_1^2(t-\theta_1)}, \\ \dfrac{d^{\rho}x_2(t)}{dt^{\rho}} = \gamma\beta\left[x_1(t-\theta_2) - \dfrac{x_1(t-\theta_2)x_2(t-\theta_1)}{1+x_1^2(t-\theta_2)}\right], \end{cases} \tag{7}$$

where $\rho \in (0, 1]$. All other coefficients admit the same implication as those in model (6). For simplicity, we let $\theta_1 = \theta_2 = \theta$, then model (7) reads as

$$\begin{cases} \dfrac{d^{\rho}x_1(t)}{dt^{\rho}} = \alpha - x_1(t-\theta) - \dfrac{4x_1(t-\theta)x_2(t-\theta)}{1+x_1^2(t-\theta)}, \\ \dfrac{d^{\rho}x_2(t)}{dt^{\rho}} = \gamma\beta\left[x_1(t-\theta) - \dfrac{x_1(t-\theta)x_2(t-\theta)}{1+x_1^2(t-\theta)}\right]. \end{cases} \tag{8}$$

In this work, we are to deal with the following three aspects: **(i)** explore the stability trait and the onset of Hopf bifurcation of model (8). **(ii)** control the stability domain and the time of generation of bifurcation for model

(8) via nonlinear delayed feedback controller. **(iii)** control the stability domain and the time of generation of bifurcation for model (8) via hybrid controller.

The basic framework of this work is given as follows. Some elementary knowledge on fractional-order dynamical system is prepared in Part 2. Part 3 explores the stability and Hopf bifurcation for system (8) and a novel delay-independent criterion on stability and bifurcation of system (8) is gained. Part 4 dealt with the control of stability domain and Hopf bifurcation of model (8) by virtue of nonlinear delayed feedback controller. Part 5 focuses on the control of stability domain and Hopf bifurcation of model (8) via hybrid controller. Part 6 executes Mathlab experiments to verify the efficiency of the acquired outcomes. Part 7 draws a concise conclusion to finish the work.

2 Elementary theory

In this segment, some essential basic theories about fractional-order differential equation are presented.

Definition 2.1. **[41]** *Define the fractional integral of order ρ of the function $g(\varepsilon)$ as follows:*

$$\mathcal{I}^{\rho} g(\varepsilon) = \frac{1}{\Gamma(\rho)} \int_{\varepsilon_0}^{\varepsilon} (\varepsilon - u)^{\rho-1} g(u) du,$$

where $\varepsilon > \varepsilon_0, \rho > 0, \Gamma(u) = \int_0^{\infty} s^{u-1} e^{-s} ds$ represents the Gamma function.

Definition 2.2. **[42]** *The Caputo fractional-order derivative of order ρ of the function $g(\varepsilon) \in ([\varepsilon_0, \infty), R)$ is defined as follows:*

$$\mathcal{D}^{\rho} g(\varepsilon) = \frac{1}{\Gamma(\iota - \rho)} \int_{\varepsilon_0}^{\varepsilon} \frac{g^{(m)}(s)}{(\varepsilon - s)^{\rho - m + 1}} ds,$$

where $\varepsilon \geq \varepsilon_0$ and m represents a positive integer $(m - 1 \leq \rho < m)$. In

particular, if $\rho \in (0,1)$*, then*

$$\mathcal{D}^{\rho} g(\varepsilon) = \frac{1}{\Gamma(1-\rho)} \int_{\varepsilon_0}^{\varepsilon} \frac{g^{'}(s)}{(\varepsilon - s)^{\rho}} ds.$$

Lemma 2.1. **[43]** *For the fractional system:* $\mathcal{D}^{\rho} x = \mathcal{A}x, x(0) = x_0$ *where* $\rho \in (0,1), x \in R^m, \mathcal{A} \in R^{m \times m}$*. Let* $u_k (k = 1, 2, \cdots, m)$ *be the root of the characteristic equation of* $\mathcal{D}^{\rho} x = \mathcal{A}x$*, then we say that system* $\mathcal{D}^{\rho} x = \mathcal{A}x$ *is locally asymptotically stable* $\Leftrightarrow |arg(u_k)| > \frac{\rho\pi}{2} (k = 1, 2, \cdots, m)$*. The system is stable* $\Leftrightarrow |arg(u_k)| > \frac{\rho\pi}{2} (k = 1, 2, \cdots, m)$ *and all critical eigenvalues obeying* $|arg(u_k)| = \frac{\rho\pi}{2} (k = 1, 2, \cdots, m)$ *own geometric multiplicity one.*

3 Bifurcation analysis

Clearly, one can obtain that model (8) admits the following unique positive equilibrium point $E(x_{1*}, x_{2*})$, where

$$\begin{cases} x_{1*} = \dfrac{\alpha}{5}, \\ x_{2*} = 1 + \dfrac{\alpha^2}{25}. \end{cases} \tag{9}$$

The linear system of model (8) at $E(x_{1*}, x_{2*})$ has the following expression:

$$\mathcal{D}^{\rho} x(t) = Ax(t - \theta), \tag{10}$$

where

$$x(t) = \begin{bmatrix} x_1(t) \\ x_2(t) \end{bmatrix}, A = \begin{bmatrix} a_1 & a_2 \\ a_3 & a_4 \end{bmatrix}, \tag{11}$$

where

$$\begin{cases} a_1 = \dfrac{8x_{1*}^2 x_{2*} - 4x_{2*}}{1 + x_{1*}^2} - 1, \\ a_2 = -\dfrac{4x_{1*}}{1 + x_{1*}^2}, \\ a_3 = \dfrac{2x_{1*}^2 x_{2*} - x_{2*}}{1 + x_{1*}^2} + 1, \\ a_4 = -\dfrac{x_{1*}}{1 + x_{1*}^2}. \end{cases} \tag{12}$$

The characteristic equation of system (10) reads as

$$\det\begin{bmatrix} s^{\rho}-a_1e^{-s\theta} & -a_2e^{-s\theta} \\ -a_3e^{-s\theta} & s^{\rho}-a_4e^{-s\theta} \end{bmatrix}=0, \tag{13}$$

which generates

$$s^{2\rho}+b_1s^{\rho}e^{-s\theta}+b_2e^{-2s\theta}=0, \tag{14}$$

where

$$\begin{cases} b_1=-(a_1+a_4), \\ b_2=a_1a_4-a_2a_3. \end{cases} \tag{15}$$

When $\theta=0$, then Eq.(14) has the following form:

$$\lambda^2+b_1\lambda+b_2=0, \tag{16}$$

If

$$(S_1)\ b_1>0, b_2>0$$

holds true, then the both roots λ_1,λ_2 of Eq. (16) satisfies $|\arg(\lambda_1)|>\frac{\rho\pi}{2}, |\arg(\lambda_2)|>\frac{\rho\pi}{2}$. According to Lemma 2.1, one gains that the positive equilibrium point $E(x_{1*},x_{2*})$ of model (8) under the delay $\theta=0$ remains locally asymptotically stability.

By (3.6), we have

$$s^{2\rho}e^{s\theta}+b_1s^{\rho}+b_2e^{-s\theta}=0. \tag{17}$$

Suppose that $s=i\phi=\phi\left(\cos\frac{\pi}{2}+i\sin\frac{\pi}{2}\right)$ is the root of Eq. (17). Then it follows from Eq.(17) that

$$\begin{aligned} &\phi^{2\rho}(\cos\rho\pi+i\sin\rho\pi)(\cos\phi\theta+i\sin\phi\theta) \\ &+b_1\phi^{\rho}\left(\cos\frac{\rho\pi}{2}+i\sin\frac{\rho\pi}{2}\right)+b_2(\cos\phi\theta-i\sin\phi\theta)=0. \end{aligned} \tag{18}$$

Then

$$\begin{cases} \left(\phi^{2\rho}\cos\rho\pi+b_2\right)\cos\phi\theta-\phi^{2\rho}\sin\rho\pi\sin\phi\theta=-b_1\phi^{\rho}\cos\dfrac{\rho\pi}{2}, \\ \phi^{2\rho}\sin\rho\pi\cos\phi\theta+\left(\phi^{2\rho}\cos\rho\pi-b_2\right)\sin\phi\theta=-b_1\phi^{\rho}\sin\dfrac{\rho\pi}{2}. \end{cases} \tag{19}$$

By (19), we have

$$\begin{cases} \cos\phi\theta = \dfrac{-b_1\phi^{3\rho}\left(\cos\frac{\rho\pi}{2}\cos\rho\pi + \sin\frac{\rho\pi}{2}\sin\rho\pi\right) + b_1b_2\phi^{\rho}\cos\frac{\rho\pi}{2}}{\phi^{4\rho} - b_2^2}, \\ \sin\phi\theta = \dfrac{-b_1\phi^{3\rho}\left(\sin\frac{\rho\pi}{2}\cos\rho\pi - \cos\frac{\rho\pi}{2}\sin\rho\pi\right) - b_1b_2\phi^{\rho}\sin\frac{\rho\pi}{2}}{\phi^{4\rho} - b_2^2}. \end{cases} \tag{20}$$

In view of $\cos^2\phi\theta + \sin^2\phi\theta = 1$, it follows from (20) that

$$\begin{aligned} &\left[b_1\phi^{3\rho}\left(\cos\frac{\rho\pi}{2}\cos\rho\pi + \sin\frac{\rho\pi}{2}\sin\rho\pi\right) - b_1b_2\phi^{\rho}\cos\frac{\rho\pi}{2}\right]^2 \\ &+ \left[b_1\phi^{3\rho}\left(\sin\frac{\rho\pi}{2}\cos\rho\pi - \cos\frac{\rho\pi}{2}\sin\rho\pi\right) + b_1b_2\phi^{\rho}\sin\frac{\rho\pi}{2}\right]^2 \\ &= \left(\phi^{4\rho} - b_2^2\right)^2, \end{aligned} \tag{21}$$

which results in

$$\phi^{8\rho} + d_1\phi^{6\rho} + d_2\phi^{4\rho} + d_3\phi^{2\rho} + d_4 = 0, \tag{22}$$

where

$$\begin{cases} d_1 = 2b_1^2, \\ d_2 = 2b_1^2b_2^2\cos\dfrac{\rho\pi}{2}\left(\cos\dfrac{\rho\pi}{2}\cos\rho\pi + \sin\dfrac{\rho\pi}{2}\sin\rho\pi\right) \\ \qquad -2b_1^2b_2^2\sin\dfrac{\rho\pi}{2}\left(\sin\dfrac{\rho\pi}{2}\cos\rho\pi - \cos\dfrac{\rho\pi}{2}\sin\rho\pi\right) - 2b_2^2, \\ d_3 = b_1^2b_2^2, \\ d_4 = b_4^2. \end{cases} \tag{23}$$

Denote

$$Q_1(\phi) = \phi^{8\rho} + d_1\phi^{6\rho} + d_2\phi^{4\rho} + d_3\phi^{2\rho} + d_4 \tag{24}$$

and

$$Q_2(\phi) = \phi^8 + d_1\phi^6 + d_2\phi^4 + d_3\phi^2 + d_4. \tag{25}$$

Lemma 3.1 *(i) If $d_i > 0 (i = 1, 2, 3)$, then Eq. (14) admits no root possessing zero real part. (ii) If there exists a constant $\mu_0 > 0$ satisfying $Q_2(\mu_0) < 0$, then Eq. (14) admits at least two couples of purely imaginary roots.*

Proof (i) Applying (14), one gains

$$\frac{dQ_1(\phi)}{d\phi} = 8\rho\phi^{8\rho-1} + 6\rho d_1\phi^{6\rho-1} + 4\rho d_2\phi^{4\rho-1} + 2\rho d_3\phi^{2\rho-1}. \tag{26}$$

Notice that $d_l > 0 (l = 1, 2, 3)$, one gets $\frac{dQ_1(\phi)}{d\phi} > 0, \forall \ \ \phi > 0$. Besides $Q_1(0) = d_4 > 0$, we understand that Eq.(22) possesses no positive real root. By the assumption (S_1), we understand that $s = 0$ is not the root of (14). The proof of (i) ends.

(ii) Obviously, $Q_2(0) = d_4 > 0, Q_2(\mu_0) < 0 (\mu_0 > 0)$ and $\lim_{\phi\to+\infty} \frac{Q_2(\phi)}{d\phi} = +\infty$, then there exist $\mu_1 \in (0, \mu_0)$ and $\mu_2 \in (\mu_0, +\infty)$ satisfying $Q_2(\mu_1) = Q_2(\mu_2) = 0$, then Eq.(22) possesses at least two positive real roots. So (14) possesses at least two couples of purely imaginary roots. The proof of (ii) ends. ■

Assume that Eq.(22) owns eight positive real roots $\phi_l (l = 1, 2, \cdots, 8)$. According to (20), one gains

$$\theta_l^j = \frac{1}{\phi_l}\left[\arccos T + 2j\pi\right], \tag{27}$$

where

$$T = \frac{-b_1\phi_l^{3\rho}\left(\cos\frac{\rho\pi}{2}\cos\rho\pi + \sin\frac{\rho\pi}{2}\sin\rho\pi\right) + b_1b_2\phi_l^{\rho}\cos\frac{\rho\pi}{2}}{\phi_l^{4\rho} - b_2^2}$$

and $j = 0, 1, 2, \cdots, l = 1, 2, \cdots, 8$. Let

$$\theta_0 = \min_{l=1,2,\cdots,8}\{\theta_l^0\}, \phi_0 = \phi|_{\theta=\theta_0}. \tag{28}$$

Now we give the following condition:

$$(S_2) \ \ A_{1R}A_{2R} + A_{1I}A_{2I} > 0,$$

where

$$\begin{cases} A_{1R} = 2\rho\phi_0^{2\rho-1}\cos\dfrac{(2\rho-1)\pi}{2} + b_1\rho\phi_0^{\rho-1}\cos\dfrac{(\rho-1)\pi}{2}\cos\phi_0\theta_0 \\ \quad +b_1\rho\phi_0^{\rho-1}\sin\dfrac{(\rho-1)\pi}{2}\sin\phi_0\theta_0, \\ A_{1I} = 2\rho\phi_0^{2\rho-1}\sin\dfrac{(2\rho-1)\pi}{2} - b_1\rho\phi_0^{\rho-1}\cos\dfrac{(\rho-1)\pi}{2}\sin\phi_0\theta_0 \\ \quad +b_1\rho\phi_0^{\rho-1}\sin\dfrac{(\rho-1)\pi}{2}\cos\phi_0\theta_0, \\ A_{2R} = b_1\phi_0^{\rho+1}\left[\cos\dfrac{(\rho+1)\pi}{2}\cos\phi_0\theta_0 + \sin\dfrac{(\rho+1)\pi}{2}\sin\phi_0\theta_0\right] \\ \quad +2b_2\phi_0\sin 2\phi_0\theta_0, \\ A_{2I} = -b_1\phi_0^{\rho+1}\left[\cos\dfrac{(\rho+1)\pi}{2}\sin\phi_0\theta_0 - \sin\dfrac{(\rho+1)\pi}{2}\cos\phi_0\theta_0\right] \\ \quad +2b_2\phi_0\cos 2\phi_0\theta_0. \end{cases} \tag{29}$$

Lemma 3.2. *Let $s(\theta) = \zeta_1(\theta) + i\zeta_2(\theta)$ be the root of Eq. (14) near $\theta = \theta_0$ satisfying $\zeta_1(\theta_0) = 0, \zeta_2(\theta_0) = \phi_0$, then $Re\left(\frac{ds}{d\theta}\right)\Big|_{\theta=\theta_0,\phi=\phi_0} > 0$.*

Proof By Eq.(14), we gain

$$\begin{aligned} &2\rho s^{2\rho-1}\frac{ds}{d\theta} + b_1\rho s^{\rho-1}e^{-s\theta}\frac{ds}{d\theta} - b_1 s^{\rho}e^{-s\theta}\left(\frac{ds}{d\theta}\theta + s\right) \\ &-2b_2e^{-2s\theta}\left(\frac{ds}{d\theta}\theta + s\right) = 0, \end{aligned} \tag{30}$$

which implies

$$\left(\frac{ds}{d\theta}\right)^{-1} = \frac{A_1(s)}{A_2(s)} - \frac{\theta}{s}, \tag{31}$$

where

$$\begin{cases} A_1(s) = 2\rho s^{2\rho-1} + b_1\rho s^{\rho-1}e^{-s\theta}, \\ A_2(s) = b_1 s^{\rho+1}e^{-s\theta} + 2b_2 s e^{-2s\theta}. \end{cases} \tag{32}$$

Then

$$\mathrm{Re}\left[\left(\frac{ds}{d\theta}\right)^{-1}\right]_{\theta=\theta_0,\phi=\phi_0} = \mathrm{Re}\left[\frac{A_1(s)}{A_2(s)}\right]_{\theta=\theta_0,\phi=\phi_0} = \frac{A_{1R}A_{2R} + A_{1I}A_{2I}}{A_{2R}^2 + A_{2I}^2}. \tag{33}$$

By (S_2), one gains

$$\mathrm{Re}\left[\left(\frac{ds}{d\theta}\right)^{-1}\right]_{\theta=\theta_0,\phi=\phi_0} > 0, \tag{34}$$

which ends the proof. ■

Using Lemma 2.1, the following outcome is established.

Theorem 3.1. *If (S_1) and (S_2) hold, then $E(x_{1*}, x_{2*})$ of model (8) remains locally asymptotically stability if $\theta \in [0, \theta_0)$ and a Hopf bifurcation of model (8) arises around $E(x_{1*}, x_{2*})$ when $\theta = \theta_0$.*

4 Bifurcation control via nonlinear delayed feedback controller

In this part, we will make use of an appropriate nonlinear delayed feedback controller to control the stability and Hopf bifurcation for model (8). Following the way in [45], we design the nonlinear delayed feedback controller as follows:

$$\nu(t) = \varrho_1[x_1(t-\theta) - x_{1*}] + \varrho_2[x_1(t-\theta) - x_{1*}]^2, \tag{35}$$

where ϱ_1, ϱ_2 represent feedback gain parameters. Adding the nonlinear delayed feedback controller $\nu(t)$ to the first equation of model (8), we gain the following fractional-order controlled Lengyel-Epstein model owing time delay:

$$\begin{cases} \dfrac{d^\rho x_1(t)}{dt^\rho} = \alpha - x_1(t-\theta) - \dfrac{4x_1(t-\theta)x_2(t-\theta)}{1+x_1^2(t-\theta)} \\ \qquad\qquad +\varrho_1[x_1(t-\theta) - x_{1*}] + \varrho_2[x_1(t-\theta) - x_{1*}]^2, \\ \dfrac{d^\rho x_2(t)}{dt^\rho} = \gamma\beta\left[x_1(t-\theta) - \dfrac{x_1(t-\theta)x_2(t-\theta)}{1+x_1^2(t-\theta)}\right]. \end{cases} \tag{36}$$

Clearly, model (36)and model (8) admit the same positive equilibrium point $E(x_{1*}, x_{2*})$. The linear system of model (36) at $E(x_{1*}, x_{2*})$ has the

following expression:

$$\mathcal{D}^{\rho}x(t) = Bx(t-\theta), \tag{37}$$

where

$$x(t) = \begin{bmatrix} x_1(t) \\ x_2(t) \end{bmatrix}, B = \begin{bmatrix} e_1 & e_2 \\ e_3 & e_4 \end{bmatrix}, \tag{38}$$

where

$$\begin{cases} e_1 = \dfrac{8x_{1*}^2 x_{2*} - 4x_{2*}}{1+x_{1*}^2} - 1 + \varrho_1 - 2\varrho_2 x_{1*}, \\ e_2 = -\dfrac{4x_{1*}}{1+x_{1*}^2}, \\ e_3 = \dfrac{2x_{1*}^2 x_{2*} - x_{2*}}{1+x_{1*}^2} + 1, \\ e_4 = -\dfrac{x_{1*}}{1+x_{1*}^2}. \end{cases} \tag{39}$$

The characteristic equation of system (37) reads as

$$\det \begin{bmatrix} s^{\rho} - e_1 e^{-s\theta} & -e_2 e^{-s\theta} \\ -e_3 e^{-s\theta} & s^{\rho} - e_4 e^{-s\theta} \end{bmatrix} = 0, \tag{40}$$

which generates

$$s^{2\rho} + f_1 s^{\rho} e^{-s\theta} + f_2 e^{-2s\theta} = 0, \tag{41}$$

where

$$\begin{cases} f_1 = -(e_1 + e_4), \\ f_2 = e_1 e_4 - e_2 e_3. \end{cases} \tag{42}$$

When $\theta = 0$, then Eq.(41) has the following form:

$$\lambda^2 + f_1 \lambda + f_2 = 0, \tag{43}$$

If

$$(S_3)\ f_1 > 0, f_2 > 0$$

holds true, then the both roots λ_1, λ_2 of Eq. (43) satisfies $|\arg(\lambda_1)| > \frac{\rho\pi}{2}, |\arg(\lambda_2)| > \frac{\rho\pi}{2}$. According to Lemma 2.1, one gains that the positive equilibrium point $E(x_{1*}, x_{2*})$ of model (36) under the delay $\theta = 0$ remains locally asymptotically stability.

By (41), we have

$$s^{2\rho}e^{s\theta} + f_1 s^{\rho} + f_2 e^{-s\theta} = 0. \tag{44}$$

Suppose that $s = i\varphi = \varphi\left(\cos\frac{\pi}{2} + i\sin\frac{\pi}{2}\right)$ is the root of Eq. (44). Then it follows from Eq.(44) that

$$\begin{aligned}&\varphi^{2\rho}(\cos\rho\pi + i\sin\rho\pi)(\cos\varphi\theta + i\sin\varphi\theta)\\&+f_1\varphi^{\rho}\left(\cos\frac{\rho\pi}{2} + i\sin\frac{\rho\pi}{2}\right) + f_2(\cos\varphi\theta - i\sin\varphi\theta) = 0.\end{aligned} \tag{45}$$

Then

$$\begin{cases}\left(\phi^{2\rho}\cos\rho\pi + f_2\right)\cos\varphi\theta - \varphi^{2\rho}\sin\rho\pi\sin\varphi\theta = -f_1\varphi^{\rho}\cos\dfrac{\rho\pi}{2},\\ \varphi^{2\rho}\sin\rho\pi\cos\varphi\theta + \left(\varphi^{2\rho}\cos\rho\pi - f_2\right)\sin\varphi\theta = -f_1\varphi^{\rho}\sin\dfrac{\rho\pi}{2}.\end{cases} \tag{46}$$

By (46), we have

$$\begin{cases}\cos\varphi\theta = \dfrac{-f_1\phi^{3\rho}\left(\cos\frac{\rho\pi}{2}\cos\rho\pi + \sin\frac{\rho\pi}{2}\sin\rho\pi\right) + f_1f_2\varphi^{\rho}\cos\frac{\rho\pi}{2}}{\varphi^{4\rho} - f_2^2},\\ \sin\varphi\theta = \dfrac{-f_1\varphi^{3\rho}\left(\sin\frac{\rho\pi}{2}\cos\rho\pi - \cos\frac{\rho\pi}{2}\sin\rho\pi\right) - f_1f_2\varphi^{\rho}\sin\frac{\rho\pi}{2}}{\varphi^{4\rho} - f_2^2}.\end{cases} \tag{47}$$

In view of $\cos^2\varphi\theta + \sin^2\varphi\theta = 1$, it follows from (47) that

$$\begin{aligned}&\left[f_1\varphi^{3\rho}\left(\cos\frac{\rho\pi}{2}\cos\rho\pi + \sin\frac{\rho\pi}{2}\sin\rho\pi\right) - f_1f_2\varphi^{\rho}\cos\frac{\rho\pi}{2}\right]^2\\&+\left[f_1\varphi^{3\rho}\left(\sin\frac{\rho\pi}{2}\cos\rho\pi - \cos\frac{\rho\pi}{2}\sin\rho\pi\right) + f_1f_2\varphi^{\rho}\sin\frac{\rho\pi}{2}\right]^2\\&= \left(\varphi^{4\rho} - f_2^2\right)^2,\end{aligned} \tag{48}$$

which results in

$$\varphi^{8\rho} + g_1\varphi^{6\rho} + g_2\varphi^{4\rho} + g_3\varphi^{2\rho} + g_4 = 0, \tag{49}$$

where

$$\begin{cases} g_1 = 2f_1^2, \\ g_2 = 2f_1^2 f_2^2 \cos\dfrac{\rho\pi}{2}\left(\cos\dfrac{\rho\pi}{2}\cos\rho\pi + \sin\dfrac{\rho\pi}{2}\sin\rho\pi\right) \\ \quad -2f_1^2 f_2^2 \sin\dfrac{\rho\pi}{2}\left(\sin\dfrac{\rho\pi}{2}\cos\rho\pi - \cos\dfrac{\rho\pi}{2}\sin\rho\pi\right) - 2f_2^2, \\ g_3 = f_1^2 f_2^2, \\ g_4 = f_4^2. \end{cases} \tag{50}$$

Denote

$$P_1(\varphi) = \varphi^{8\rho} + g_1\varphi^{6\rho} + g_2\varphi^{4\rho} + g_3\varphi^{2\rho} + g_4 \tag{51}$$

and

$$P_2(\varphi) = \varphi^8 + g_1\varphi^6 + g_2\varphi^4 + g_3\varphi^2 + g_4. \tag{52}$$

Lemma 4.1 *(i) If $f_i > 0 (i = 1, 2, 3)$, then Eq. (41) admits no root possessing zero real part. (ii) If there exists a constant $v_0 > 0$ satisfying $P_2(v_0) < 0$, then Eq. (41) admits at least two couples of purely imaginary roots.*

Proof (i) Applying (41), one gains

$$\frac{dP_1(\varphi)}{d\varphi} = 8\rho\varphi^{8\rho-1} + 6\rho f_1\varphi^{6\rho-1} + 4\rho f_2\varphi^{4\rho-1} + 2\rho f_3\varphi^{2\rho-1}. \tag{53}$$

Notice that $f_l > 0 (l = 1, 2, 3)$, one gets $\frac{dP_1(\varphi)}{d\varphi} > 0, \forall \ \varphi > 0$. Besides $P_1(0) = f_4 > 0$, we understand that Eq.(49) possesses no positive real root. By the assumption (S_3), we understand that $s = 0$ is not the root of (41). The proof of (i) ends.

(ii) Obviously, $P_2(0) = f_4 > 0, P_2(v_0) < 0 (v_0 > 0)$ and $\lim_{\varphi\to+\infty}\frac{P_2(\varphi)}{d\varphi} = +\infty$, then there exist $v_1 \in (0, v_0)$ and $v_2 \in (v_0, +\infty)$ satisfying $P_2(v_1) = P_2(v_2) = 0$, then Eq.(49) possesses at least two positive real roots. So (41) possesses at least two couples of purely imaginary roots. The proof of (ii) ends. ■

Assume that Eq.(49) owns eight positive real roots $\varphi_l (l = 1, 2, \cdots, 8)$.

According to (47), one gains

$$\theta_m^i = \frac{1}{\varphi_m}\left[\arccos V + 2i\pi\right], \tag{54}$$

where

$$V = \frac{-f_1\varphi_m^{3\rho}\left(\cos\frac{\rho\pi}{2}\cos\rho\pi + \sin\frac{\rho\pi}{2}\sin\rho\pi\right) + f_1 f_2\varphi_m^{\rho}\cos\frac{\rho\pi}{2}}{\varphi_m^{4\rho} - f_2^2}$$

and $i = 0, 1, 2, \cdots, m = 1, 2, \cdots, 8$. Let

$$\theta_* = \min_{m=1,2,\cdots,8}\{\theta_m^0\}, \varphi_0 = \varphi|_{\theta=\theta_*}. \tag{55}$$

Next we give the following condition:

$$(S_4)\quad B_{1R}B_{2R} + B_{1I}B_{2I} > 0,$$

where

$$\begin{cases} B_{1R} = 2\rho\varphi_0^{2\rho-1}\cos\dfrac{(2\rho-1)\pi}{2} + f_1\rho\varphi_0^{\rho-1}\cos\dfrac{(\rho-1)\pi}{2}\cos\varphi_0\theta_* \\ \qquad +f_1\rho\varphi_0^{\rho-1}\sin\dfrac{(\rho-1)\pi}{2}\sin\varphi_0\theta_*, \\ B_{1I} = 2\rho\varphi_0^{2\rho-1}\sin\dfrac{(2\rho-1)\pi}{2} - f_1\rho\varphi_0^{\rho-1}\cos\dfrac{(\rho-1)\pi}{2}\sin\varphi_0\theta_* \\ \qquad +f_1\rho\varphi_0^{\rho-1}\sin\dfrac{(\rho-1)\pi}{2}\cos\varphi_0\theta_*, \\ B_{2R} = f_1\varphi_0^{\rho+1}\left[\cos\dfrac{(\rho+1)\pi}{2}\cos\varphi_0\theta_* + \sin\dfrac{(\rho+1)\pi}{2}\sin\varphi_0\theta_*\right] \\ \qquad +2f_2\varphi_0\sin 2\varphi_0\theta_*, \\ B_{2I} = -f_1\varphi_0^{\rho+1}\left[\cos\dfrac{(\rho+1)\pi}{2}\sin\varphi_0\theta_* - \sin\dfrac{(\rho+1)\pi}{2}\cos\varphi_0\theta_*\right] \\ \qquad +2f_2\varphi_0\cos 2\varphi_0\theta_*. \end{cases} \tag{56}$$

Lemma 3.2. *Let $s(\theta) = \xi_1(\theta) + i\xi_2(\theta)$ be the root of Eq. (41) near $\theta = \theta_*$ satisfying $\xi_1(\theta_*) = 0, \xi_2(\theta_*) = \varphi_0$, then $Re\left(\frac{ds}{d\theta}\right)\Big|_{\theta=\theta_*,\varphi=\varphi_0} > 0$.*

Proof By Eq.(41), we gain

$$2\rho s^{2\rho-1}\frac{ds}{d\theta}+f_1\rho s^{\rho-1}e^{-s\theta}\frac{ds}{d\theta}-f_1 s^{\rho}e^{-s\theta}\left(\frac{ds}{d\theta}\theta+s\right)$$
$$-2f_2e^{-2s\theta}\left(\frac{ds}{d\theta}\theta+s\right)=0, \tag{57}$$

which implies

$$\left(\frac{ds}{d\theta}\right)^{-1}=\frac{B_1(s)}{B_2(s)}-\frac{\theta}{s}, \tag{58}$$

where

$$\begin{cases} B_1(s)=2\rho s^{2\rho-1}+f_1\rho s^{\rho-1}e^{-s\theta}, \\ B_2(s)=f_1s^{\rho+1}e^{-s\theta}+2f_2se^{-2s\theta}. \end{cases} \tag{59}$$

Then

$$\mathrm{Re}\left[\left(\frac{ds}{d\theta}\right)^{-1}\right]_{\theta=\theta_*,\varphi=\varphi_0}=\mathrm{Re}\left[\frac{B_1(s)}{B_2(s)}\right]_{\theta=\theta_*,\varphi=\varphi_0}=\frac{B_{1R}B_{2R}+B_{1I}B_{2I}}{B_{2R}^2+B_{2I}^2}. \tag{60}$$

By (S_4), one gains

$$\mathrm{Re}\left[\left(\frac{ds}{d\theta}\right)^{-1}\right]_{\theta=\theta_*,\varphi=\varphi_0}>0, \tag{61}$$

which ends the proof. ■

Using Lemma 2.1, the following outcome is established.

Theorem 4.1. *If (S_3) and (S_4) hold, then $E(x_{1*},x_{2*})$ of model (36) remains locally asymptotically stability if $\theta\in[0,\theta_*)$ and a Hopf bifurcation of model (36) arises around $E(x_{1*},x_{2*})$ when $\theta=\theta_*$.*

5 Bifurcation control via hybrid control

In this section, we are to design a proper hybrid controller consisting of state feedback and parameter perturbation to control the stability and Hopf bifurcation of model (8). Following the idea of [46, 47], we get the following fractional-order controlled Lengyel-Epstein model owing time de-

lay:

$$\begin{cases} \dfrac{d^{\rho}x_1(t)}{dt^{\rho}} = \sigma_1\left[\alpha - x_1(t-\theta) - \dfrac{4x_1(t-\theta)x_2(t-\theta)}{1+x_1^2(t-\theta)}\right] \\ \qquad\qquad +\sigma_2[x_1(t-\theta) - x_{1*}], \\ \dfrac{d^{\rho}x_2(t)}{dt^{\rho}} = \sigma_1\left\{\gamma\beta\left[x_1(t-\theta) - \dfrac{x_1(t-\theta)x_2(t-\theta)}{1+x_1^2(t-\theta)}\right]\right\} \\ \qquad\qquad +\sigma_2[x_2(t-\theta) - x_{2*}], \end{cases} \tag{62}$$

where σ_1, σ_2 stands for feedback gain parameters. Model (62) and model (8) own the same positive equilibrium point $E(x_{1*}, x_{2*})$. The linear system of model (62) around $E(x_{1*}, x_{2*})$ takes the form:

$$\mathcal{D}^{\rho}x(t) = Dx(t-\theta), \tag{63}$$

where

$$x(t) = \begin{bmatrix} x_1(t) \\ x_2(t) \end{bmatrix}, D = \begin{bmatrix} k_1 & k_2 \\ k_3 & k_4 \end{bmatrix}, \tag{64}$$

where

$$\begin{cases} k_1 = \sigma_1\left(\dfrac{8x_{1*}^2x_{2*} - 4x_{2*}}{1+x_{1*}^2} - 1\right) + \sigma_2, \\ k_2 = -\dfrac{4x_{1*}\sigma_1}{1+x_{1*}^2}, \\ k_3 = \sigma_1\left(\dfrac{2x_{1*}^2x_{2*} - x_{2*}}{1+x_{1*}^2} + 1\right), \\ k_4 = -\dfrac{x_{1*}\sigma_1}{1+x_{1*}^2} + \sigma_2. \end{cases} \tag{65}$$

The characteristic equation of system (63) reads as

$$\det\begin{bmatrix} s^{\rho} - k_1e^{-s\theta} & -k_2e^{-s\theta} \\ -k_3e^{-s\theta} & s^{\rho} - k_4e^{-s\theta} \end{bmatrix} = 0, \tag{66}$$

which generates

$$s^{2\rho} + l_1s^{\rho}e^{-s\theta} + l_2e^{-2s\theta} = 0, \tag{67}$$

where

$$\begin{cases} l_1 = -(k_1 + k_4), \\ l_2 = k_1k_4 - k_2k_3. \end{cases} \tag{68}$$

When $\theta = 0$, then Eq.(67) has the following form:

$$\lambda^2 + l_1\lambda + l_2 = 0, \tag{69}$$

If

$$(S_5)\ l_1 > 0, l_2 > 0$$

holds true, then the both roots λ_1, λ_2 of Eq. (69) satisfies $|\arg(\lambda_1)| > \frac{\rho\pi}{2}, |\arg(\lambda_2)| > \frac{\rho\pi}{2}$. According to Lemma 2.1, one gains that the positive equilibrium point $E(x_{1*}, x_{2*})$ of model (62) under the delay $\theta = 0$ remains locally asymptotically stability.

By (5.6), we have

$$s^{2\rho}e^{s\theta} + l_1 s^{\rho} + l_2 e^{-s\theta} = 0. \tag{70}$$

Suppose that $s = i\psi = \psi\left(\cos\frac{\pi}{2} + i\sin\frac{\pi}{2}\right)$ is the root of Eq. (70). Then it follows from Eq.(70) that

$$\begin{aligned} &\psi^{2\rho}(\cos\rho\pi + i\sin\rho\pi)(\cos\phi\theta + i\sin\phi\theta) \\ &+l_1\psi^{\rho}\left(\cos\frac{\rho\pi}{2} + i\sin\frac{\rho\pi}{2}\right) + l_2(\cos\psi\theta - i\sin\psi\theta) = 0. \end{aligned} \tag{71}$$

Then

$$\begin{cases} \left(\psi^{2\rho}\cos\rho\pi + l_2\right)\cos\psi\theta - \psi^{2\rho}\sin\rho\pi\sin\psi\theta = -l_1\psi^{\rho}\cos\dfrac{\rho\pi}{2}, \\ \psi^{2\rho}\sin\rho\pi\cos\psi\theta + \left(\psi^{2\rho}\cos\rho\pi - l_2\right)\sin\psi\theta = -l_1\psi^{\rho}\sin\dfrac{\rho\pi}{2}. \end{cases} \tag{72}$$

By (72), we have

$$\begin{cases} \cos\psi\theta = \dfrac{-l_1\psi^{3\rho}\left(\cos\frac{\rho\pi}{2}\cos\rho\pi + \sin\frac{\rho\pi}{2}\sin\rho\pi\right) + l_1 l_2\psi^{\rho}\cos\frac{\rho\pi}{2}}{\psi^{4\rho} - l_2^2}, \\ \sin\psi\theta = \dfrac{-l_1\phi^{3\rho}\left(\sin\frac{\rho\pi}{2}\cos\rho\pi - \cos\frac{\rho\pi}{2}\sin\rho\pi\right) - l_1 l_2\psi^{\rho}\sin\frac{\rho\pi}{2}}{\psi^{4\rho} - l_2^2}. \end{cases} \tag{73}$$

In view of $\cos^2\psi\theta + \sin^2\psi\theta = 1$, it follows from (73) that

$$\begin{aligned}&\left[l_1\psi^{3\rho}\left(\cos\frac{\rho\pi}{2}\cos\rho\pi + \sin\frac{\rho\pi}{2}\sin\rho\pi\right) - l_1l_2\psi^{\rho}\cos\frac{\rho\pi}{2}\right]^2\\&+\left[l_1\psi^{3\rho}\left(\sin\frac{\rho\pi}{2}\cos\rho\pi - \cos\frac{\rho\pi}{2}\sin\rho\pi\right) + l_1l_2\psi^{\rho}\sin\frac{\rho\pi}{2}\right]^2\\&=\left(\psi^{4\rho} - l_2^2\right)^2,\end{aligned} \tag{74}$$

which results in

$$\psi^{8\rho} + \tau_1\psi^{6\rho} + \tau_2\psi^{4\rho} + \tau_3\psi^{2\rho} + \tau_4 = 0, \tag{75}$$

where

$$\begin{cases}\tau_1 = 2l_1^2,\\ \tau_2 = 2l_1^2l_2^2\cos\dfrac{\rho\pi}{2}\left(\cos\dfrac{\rho\pi}{2}\cos\rho\pi + \sin\dfrac{\rho\pi}{2}\sin\rho\pi\right)\\ \qquad -2l_1^2l_2^2\sin\dfrac{\rho\pi}{2}\left(\sin\dfrac{\rho\pi}{2}\cos\rho\pi - \cos\dfrac{\rho\pi}{2}\sin\rho\pi\right) - 2l_2^2,\\ \tau_3 = l_1^2l_2^2,\\ \tau_4 = l_4^2.\end{cases} \tag{76}$$

Denote

$$T_1(\psi) = \psi^{8\rho} + \tau_1\psi^{6\rho} + \tau_2\psi^{4\rho} + \tau_3\psi^{2\rho} + \tau_4 \tag{77}$$

and

$$T_2(\psi) = \psi^8 + \tau_1\psi^6 + \tau_2\psi^4 + \tau_3\psi^2 + \tau_4. \tag{78}$$

Lemma 5.1 *(i) If $\tau_i > 0 (i = 1, 2, 3)$, then Eq. (67) admits no root possessing zero real part. (ii) If there exists a constant $u_0 > 0$ satisfying $T_2(u_0) < 0$, then Eq. (67) admits at least two couples of purely imaginary roots.*

Proof (i) Applying (67), one gains

$$\frac{dT_1(\psi)}{d\psi} = 8\rho\psi^{8\rho-1} + 6\rho l_1\psi^{6\rho-1} + 4\rho l_2\psi^{4\rho-1} + 2\rho l_3\psi^{2\rho-1}. \tag{79}$$

Notice that $\tau_l > 0 (l = 1, 2, 3)$, one gets $\frac{dT_1(\psi)}{d\psi} > 0, \forall \quad \psi > 0$. Besides $T_1(0) = \tau_4 > 0$, we understand that Eq.(75) possesses no positive real

root. By the assumption (S_5), we understand that $s = 0$ is not the root of (67). The proof of (i) ends.

(ii) Obviously, $T_2(0) = \tau_4 > 0, T_2(u_0) < 0 (u_0 > 0)$ and $\lim_{\psi\to+\infty} \frac{T_2(\psi)}{d\psi} = +\infty$, then there exist $u_1 \in (0, u_0)$ and $u_2 \in (u_0, +\infty)$ satisfying $T_2(u_1) = T_2(u_2) = 0$, then Eq.(75) possesses at least two positive real roots. So (67) possesses at least two couples of purely imaginary roots. The proof of (ii) ends. ■

Assume that Eq.(75) owns eight positive real roots $\psi_l (l = 1, 2, \cdots, 8)$. According to (5.12), one gains

$$\theta_\iota^n = \frac{1}{\psi_\iota} \left[\arccos S + 2n\pi\right], \tag{80}$$

where

$$S = \frac{-l_1\psi_\iota^{3\rho}\left(\cos\frac{\rho\pi}{2}\cos\rho\pi + \sin\frac{\rho\pi}{2}\sin\rho\pi\right) + l_1 l_2\psi_\iota^{\rho}\cos\frac{\rho\pi}{2}}{\psi_\iota^{4\rho} - l_2^2}$$

and $n = 0, 1, 2, \cdots, \iota = 1, 2, \cdots, 8$. Let

$$\theta_\diamond = \min_{\iota=1,2,\cdots,8}\{\theta_\iota^0\}, \psi_0 = \psi|_{\theta=\theta_\diamond}. \tag{81}$$

Now we present the following assumption:

$$(S_6) \quad C_{1R}C_{2R} + C_{1I}C_{2I} > 0,$$

where

$$\begin{cases} C_{1R} = 2\rho\psi_0^{2\rho-1}\cos\dfrac{(2\rho-1)\pi}{2} + l_1\rho\psi_0^{\rho-1}\cos\dfrac{(\rho-1)\pi}{2}\cos\psi_0\theta_\diamond \\ \quad +l_1\rho\psi_0^{\rho-1}\sin\dfrac{(\rho-1)\pi}{2}\sin\psi_0\theta_\diamond, \\ C_{1I} = 2\rho\psi_0^{2\rho-1}\sin\dfrac{(2\rho-1)\pi}{2} - l_1\rho\psi_0^{\rho-1}\cos\dfrac{(\rho-1)\pi}{2}\sin\psi_0\theta_\diamond \\ \quad +l_1\rho\psi_0^{\rho-1}\sin\dfrac{(\rho-1)\pi}{2}\cos\psi_0\theta_\diamond, \\ C_{2R} = l_1\psi_0^{\rho+1}\left[\cos\dfrac{(\rho+1)\pi}{2}\cos\psi_0\theta_0 + \sin\dfrac{(\rho+1)\pi}{2}\sin\psi_0\theta_\diamond\right] \\ \quad +2l_2\psi_0\sin 2\phi_0\theta_\diamond, \\ C_{2I} = -l_1\psi_0^{\rho+1}\left[\cos\dfrac{(\rho+1)\pi}{2}\sin\psi_0\theta_0 - \sin\dfrac{(\rho+1)\pi}{2}\cos\psi_0\theta_\diamond\right] \\ \quad +2l_2\psi_0\cos 2\psi_0\theta_\diamond. \end{cases} \tag{82}$$

Lemma 5.2. *Let $s(\theta) = \eta_1(\theta) + i\eta_2(\theta)$ be the root of Eq. (67) near $\theta = \theta_\diamond$ satisfying $\eta_1(\theta_\diamond) = 0, \eta_2(\theta_\diamond) = \psi_0$, then $Re\left(\frac{ds}{d\theta}\right)\Big|_{\theta=\theta_\diamond,\psi=\psi_0} > 0$.*

Proof By Eq.(67), we gain

$$\begin{aligned} &2\rho s^{2\rho-1}\frac{ds}{d\theta} + l_1\rho s^{\rho-1}e^{-s\theta}\frac{ds}{d\theta} - l_1 s^\rho e^{-s\theta}\left(\frac{ds}{d\theta}\theta + s\right) \\ &-2l_2 e^{-2s\theta}\left(\frac{ds}{d\theta}\theta + s\right) = 0, \end{aligned} \tag{83}$$

which implies

$$\left(\frac{ds}{d\theta}\right)^{-1} = \frac{C_1(s)}{C_2(s)} - \frac{\theta}{s}, \tag{84}$$

where

$$\begin{cases} C_1(s) = 2\rho s^{2\rho-1} + l_1\rho s^{\rho-1}e^{-s\theta}, \\ C_2(s) = l_1 s^{\rho+1}e^{-s\theta} + 2l_2 s e^{-2s\theta}. \end{cases} \tag{85}$$

Then

$$\mathrm{Re}\left[\left(\frac{ds}{d\theta}\right)^{-1}\right]_{\theta=\theta_\diamond,\psi=\psi_0} = \mathrm{Re}\left[\frac{C_1(s)}{C_2(s)}\right]_{\theta=\theta_\diamond,\psi=\psi_0} = \frac{C_{1R}C_{2R} + C_{1I}C_{2I}}{C_{2R}^2 + C_{2I}^2}. \tag{86}$$

By (S_2), one gains

$$\mathrm{Re}\left[\left(\frac{ds}{d\theta}\right)^{-1}\right]_{\theta=\theta_\diamond,\psi=\psi_0} > 0, \tag{87}$$

which ends the proof. ■

Using Lemma 2.1, the following outcome is established.

Theorem 5.1. *If (S_5) and (S_6) hold, then $E(x_{1*}, x_{2*})$ of model (62) remains locally asymptotically stability if $\theta \in [0, \theta_\diamond)$ and a Hopf bifurcation of model (62) arises around $E(x_{1*}, x_{2*})$ when $\theta = \theta_\diamond$.*

6 Matlab experiments

Example 6.1. Consider the following fractional-order Lengyel-Epstein model owing time delay:

$$\begin{cases} \dfrac{d^{0.93}x_1(t)}{dt^{0.93}} = 5 - x_1(t-\theta) - \dfrac{4x_1(t-\theta)x_2(t-\theta)}{1+x_1^2(t-\theta)}, \\ \dfrac{d^{0.93}x_2(t)}{dt^{0.93}} = 1 \times 3\left[x_1(t-\theta) - \dfrac{x_1(t-\theta)x_2(t-\theta)}{1+x_1^2(t-\theta)}\right]. \end{cases} \tag{88}$$

One can lightly gain that model (88) admits the unique positive equilibrium point $E(x_{1*}, x_{2*}) = E(1, 2)$. The two hypotheses (S_1) and (S_2) of Theorem 3.1 are met. By exploiting Matlab software, we can acquire $\phi_0 = 7.0913, \theta_0 = 0.2$. To verify the rationality of the chief outcomes of Theorem 4.1, we select both delay numbers. Firstly, let $\theta = 0.16$ which implies that $\theta < \theta_0 = 0.2$, e.g., θ lies in the domain $[0, \theta_0)$. For this situation, the Matlab experiment outcomes are presented in Figures 1-4. Clearly, Figures 1-4 show that the concentration of the first chemical reactant x_1 will tend to 1 and the concentration of the second chemical reactant x_2 will tend to 2 with the increase of time t. Secondly, let $\theta = 0.22$ which implies that $\theta > \theta_0 = 0.2$, e.g., θ crosses the threshold value θ_0. For this situation, the Matlab experiment outcomes are presented in Figures 5-8. Clearly, Figures 5-8 show that the concentration of the first chemical reactant x_1 will keep a vibration level near 1 and the concentration of the

second chemical reactant x_2 will keep a vibration level near 2. In other words, model (88) will generate a Hopf bifurcation (e.g., a limit cycle) around the positive equilibrium point $E(1,2)$. Moreover, we also draw the bifurcation diagrams to display the bifurcation value $\theta_0 = 0.2$(see Figures 9-10).

Example 6.2. Consider the following fractional-order controlled Lengyel-Epstein model owing time delay:

$$\begin{cases} \dfrac{d^{0.93}x_1(t)}{dt^{0.93}} = 5 - x_1(t-\theta) - \dfrac{4x_1(t-\theta)x_2(t-\theta)}{1+x_1^2(t-\theta)} \\ \qquad\qquad +\varrho_1[x_1(t-\theta)-x_{1*}] + \varrho_2[x_1(t-\theta)-x_{1*}]^2, \\ \dfrac{d^{0.93}x_2(t)}{dt^{0.93}} = 1\times 3\left[x_1(t-\theta) - \dfrac{x_1(t-\theta)x_2(t-\theta)}{1+x_1^2(t-\theta)}\right]. \end{cases} \tag{89}$$

One can lightly gain that model (89) admits the unique positive equilibrium point $E(x_{1*}, x_{2*}) = E(1,2)$. Let $\varrho_1 = -0.2, \varrho_2 = 0.7$. The two hypotheses (S_3) and (S_4) of Theorem 4.1 are met. By exploiting Matlab software, we can acquire $\varphi_0 = 5.4322, \theta_* = 0.27$. To verify the rationality of the chief outcomes of Theorem 4.1, we select both delay numbers. Firstly, let $\theta = 0.2$ which implies that $\theta < \theta_* = 0.27$, e.g., θ lies in the domain $[0, \theta_*)$. For this situation, the Matlab experiment outcomes are presented in Figures 11-14. Clearly, Figures 11-14 show that the concentration of the first chemical reactant x_1 will tend to 1 and the concentration of the second chemical reactant x_2 will tend to 2 with the increase of time t. Secondly, let $\theta = 0.32$ which implies that $\theta > \theta_0 = 0.27$, e.g., θ crosses the threshold value θ_*. For this situation, the Matlab experiment outcomes are presented in Figures 15-18. Clearly, Figures 15-18 show that the concentration of the first chemical reactant x_1 will keep a vibration level near 1 and the concentration of the second chemical reactant x_2 will keep a vibration level near 2. In other words, model (89) will generate a Hopf bifurcation (e.g., a limit cycle) around the positive equilibrium point $E(1,2)$. Moreover, we also draw the bifurcation diagrams to display the bifurcation value $\theta_* = 0.27$(see Figures 19-20).

Example 6.3. Consider the following fractional-order controlled Lengyel-

Epstein model owing time delay:

$$\begin{cases} \dfrac{d^{0.93}x_1(t)}{dt^{\rho}} = \sigma_1 \left[3 - x_1(t-\theta) - \dfrac{4x_1(t-\theta)x_2(t-\theta)}{1+x_1^2(t-\theta)}\right] \\ \qquad\qquad +\sigma_2[x_1(t-\theta) - x_{1*}], \\ \dfrac{d^{0.93}x_2(t)}{dt^{\rho}} = \sigma_1 \left\{1 \times 3 \left[x_1(t-\theta) - \dfrac{x_1(t-\theta)x_2(t-\theta)}{1+x_1^2(t-\theta)}\right]\right\} \\ \qquad\qquad +\sigma_2[x_2(t-\theta) - x_{2*}]. \end{cases} \tag{90}$$

One can lightly gain that model (90) admits the unique positive equilibrium point $E(x_{1*}, x_{2*}) = E(1, 2)$. Let $\sigma_1 = 1.2, \sigma_2 = 0.8$. The two hypotheses (S_5) and (S_6) of Theorem 5.1 are met. By exploiting Matlab software, we can acquire $\psi_0 = 6.0093, \theta_* = 0.141$. To verify the rationality of the chief outcomes of Theorem 5.1, we select both delay numbers. Firstly, let $\theta = 0.135$ which implies that $\theta < \theta_\diamond = 0.141$, e.g., θ lies in the domain $[0, \theta_\diamond)$. For this situation, the Matlab experiment outcomes are presented in Figures 21-24. Clearly, Figures 21-24 show that the concentration of the first chemical reactant x_1 will tend to 1 and the concentration of the second chemical reactant x_2 will tend to 2 with the increase of time t. Secondly, let $\theta = 0.146$ which implies that $\theta > \theta_\diamond = 0.141$, e.g., θ crosses the threshold value $\theta_\diamond$. For this situation, the Matlab experiment outcomes are presented in Figures 25-28. Clearly, Figures 25-28 show that the concentration of the first chemical reactant x_1 will keep a vibration level near 1 and the concentration of the second chemical reactant x_2 will keep a vibration level near 2. In other words, model (90) will generate a Hopf bifurcation (e.g., a limit cycle) around the positive equilibrium point $E(1, 2)$. Moreover, we also draw the bifurcation diagrams to display the bifurcation value $\theta_\diamond = 0.141$(see Figures 29-30).

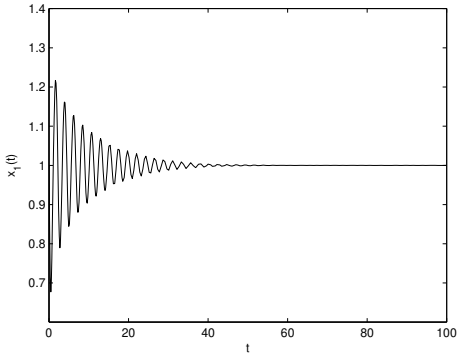

Figure 1. Matlab experiment outcomes of model (88) under the delay $\theta = 0.16 < \theta_0 = 0.2$. The positive equilibrium point $E(1, 2)$ keeps locally asymptotically stability. The x-axis represents the time t and the y-axis represents the variable $x_1(t)$.

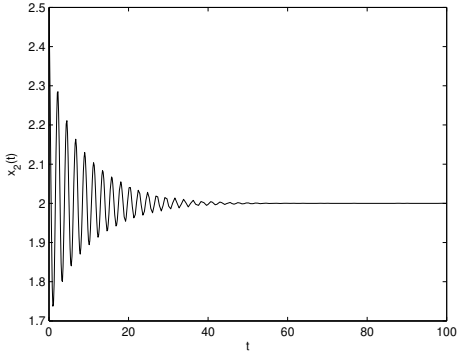

Figure 2. Matlab experiment outcomes of model (88) under the delay $\theta = 0.16 < \theta_0 = 0.2$. The positive equilibrium point $E(1, 2)$ keeps locally asymptotically stability. The x-axis represents the time t and the y-axis represents the variable $x_2(t)$.

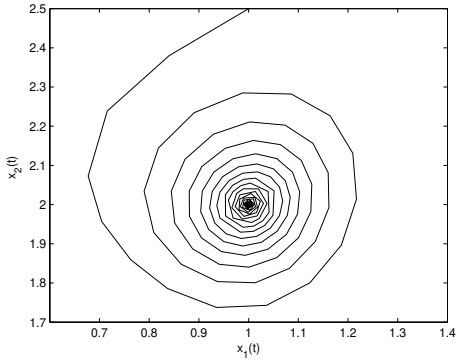

Figure 3. Matlab experiment outcomes of model (88) under the delay $\theta = 0.16 < \theta_0 = 0.2$. The positive equilibrium point $E(1, 2)$ keeps locally asymptotically stability. The x-axis represents the time $x_1(t)$ and the y-axis represents the variable $x_2(t)$.

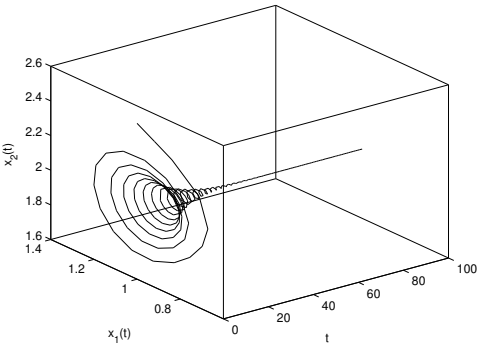

Figure 4. Matlab experiment outcomes of model (88) under the delay $\theta = 0.16 < \theta_0 = 0.2$. The positive equilibrium point $E(1, 2)$ keeps locally asymptotically stability. The x-axis represents the time t, the y-axis represents the variable $x_1(t)$ and the z-axis represents the variable $x_2(t)$.

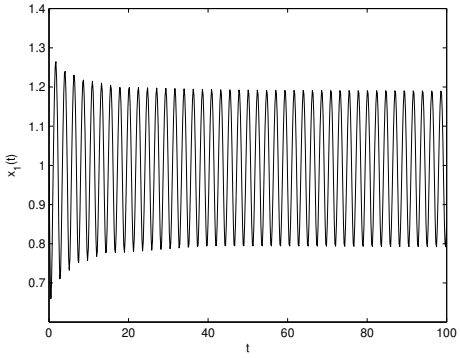

Figure 5. Matlab experiment outcomes of model (88) under the delay $\theta = 0.22 > \theta_0 = 0.2$. Hopf bifurcation takes placer around the positive equilibrium point $E(1, 2)$. The x-axis represents the time t and the y-axis represents the variable $x_1(t)$.

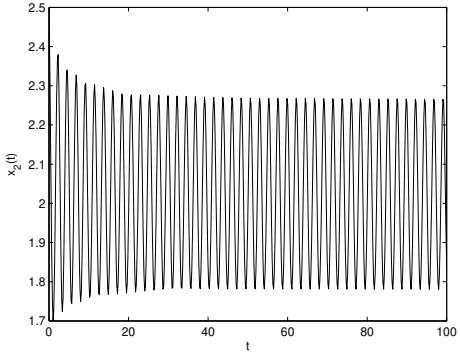

Figure 6. Matlab experiment outcomes of model (88) under the delay $\theta = 0.22 > \theta_0 = 0.2$. Hopf bifurcation takes placer around the positive equilibrium point $E(1, 2)$. The x-axis represents the time t and the y-axis represents the variable $x_2(t)$.

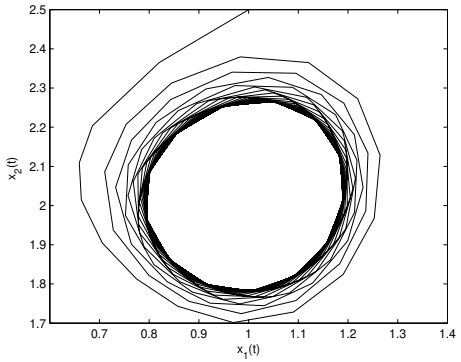

Figure 7. Matlab experiment outcomes of model (6.1) under the delay $\theta = 0.22 > \theta_0 = 0.2$. Hopf bifurcation takes placer around the positive equilibrium point $E(1, 2)$. The x-axis represents the time $x_1(t)$ and the y-axis represents the variable $x_2(t)$.

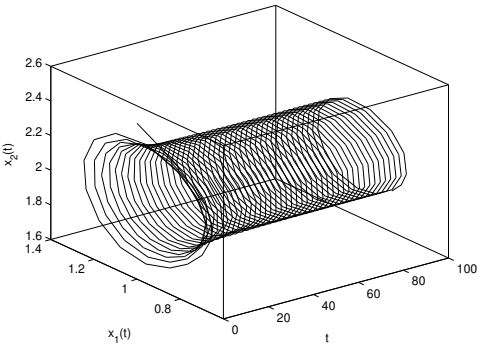

Figure 8. Matlab experiment outcomes of model (88) under the delay $\theta = 0.22 > \theta_0 = 0.2$. Hopf bifurcation takes placer around the positive equilibrium point $E(1, 2)$. The x-axis represents the time t, the y-axis represents the variable $x_1(t)$ and the z-axis represents the variable $x_2(t)$.

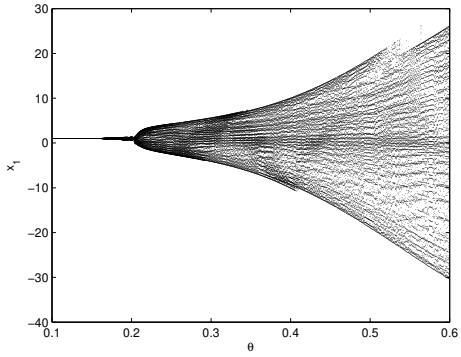

Figure 9. Bifurcation diagram of model (88): the relationship of t and x_1. The bifurcation value of model (88) is about 0.2.

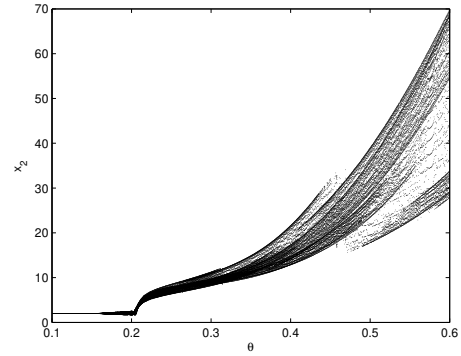

Figure 10. Bifurcation diagram of model (88): the relationship of t and x_2. The bifurcation value of model (88) is about 0.2.

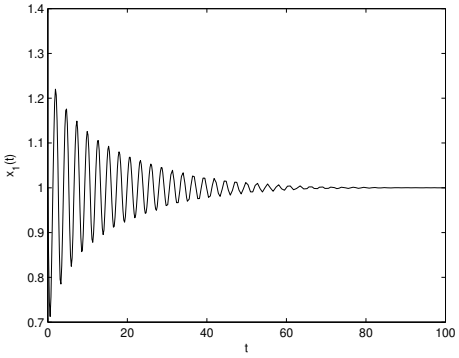

Figure 11. Matlab experiment outcomes of model (89) under the delay $\theta = 0.2 < \theta_* = 0.27$. The positive equilibrium point $E(1, 2)$ keeps locally asymptotically stability. The x-axis represents the time t and the y-axis represents the variable $x_1(t)$.

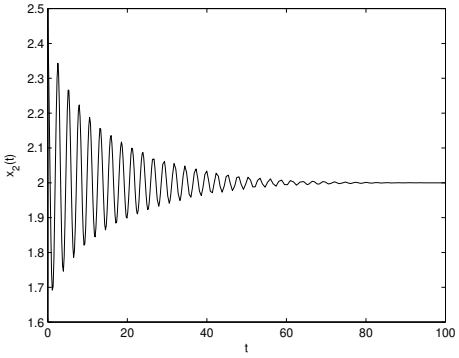

Figure 12. Matlab experiment outcomes of model (89) under the delay $\theta = 0.2 < \theta_* = 0.27$. The positive equilibrium point $E(1, 2)$ keeps locally asymptotically stability. The x-axis represents the time t and the y-axis represents the variable $x_2(t)$.

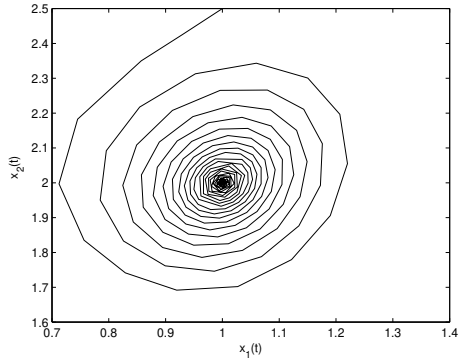

Figure 13. Matlab experiment outcomes of model (89) under the delay $\theta = 0.2 < \theta_* = 0.27$. The positive equilibrium point $E(1, 2)$ keeps locally asymptotically stability. The x-axis represents the time $x_1(t)$ and the y-axis represents the variable $x_2(t)$.

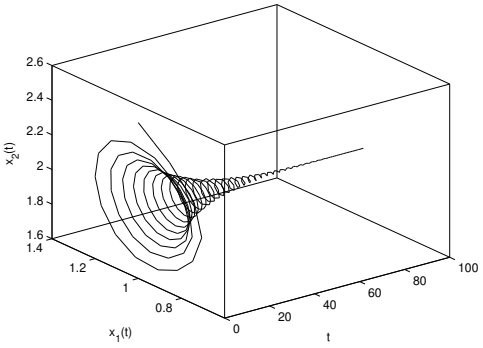

Figure 14. Matlab experiment outcomes of model (89) under the delay $\theta = 0.2 < \theta_* = 0.27$. The positive equilibrium point $E(1, 2)$ keeps locally asymptotically stability. The x-axis represents the time t, the y-axis represents the variable $x_1(t)$ and the z-axis represents the variable $x_2(t)$.

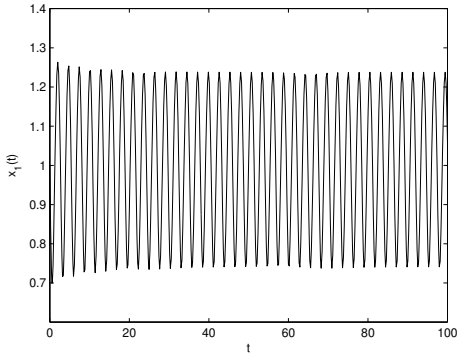

Figure 15. Matlab experiment outcomes of model (89) under the delay $\theta = 0.32 > \theta_* = 0.27$. Hopf bifurcation takes placer around the positive equilibrium point $E(1, 2)$. The x-axis represents the time t and the y-axis represents the variable $x_1(t)$.

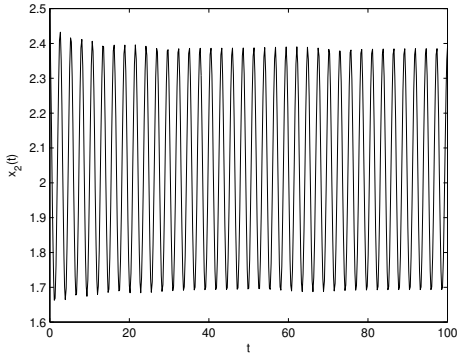

Figure 16. Matlab experiment outcomes of model (89) under the delay $\theta = 0.32 > \theta_* = 0.27$. Hopf bifurcation takes placer around the positive equilibrium point $E(1, 2)$. The x-axis represents the time t and the y-axis represents the variable $x_2(t)$.

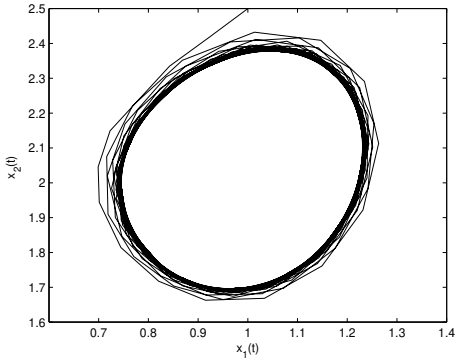

Figure 17. Matlab experiment outcomes of model (89) under the delay $\theta = 0.32 > \theta_* = 0.27$. Hopf bifurcation takes placer around the positive equilibrium point $E(1, 2)$. The x-axis represents the time $x_1(t)$ and the y-axis represents the variable $x_2(t)$.

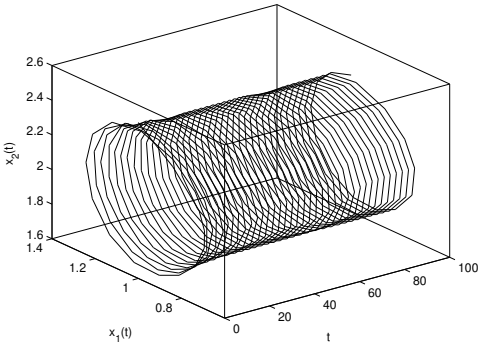

Figure 18. Matlab experiment outcomes of model (89) under the delay $\theta = 0.32 > \theta_* = 0.27$. Hopf bifurcation takes placer around the positive equilibrium point $E(1, 2)$. The x-axis represents the time t, the y-axis represents the variable $x_1(t)$ and the z-axis represents the variable $x_2(t)$.

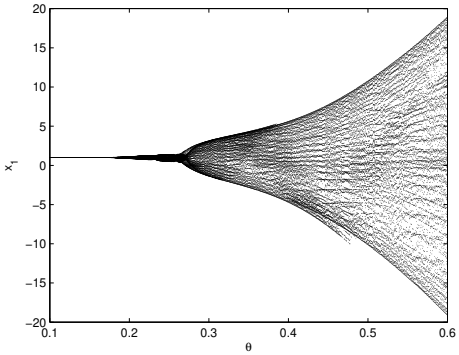

Figure 19. Bifurcation diagram of model (89): the relationship of t and x_1. The bifurcation value of model (89) is about 0.27.

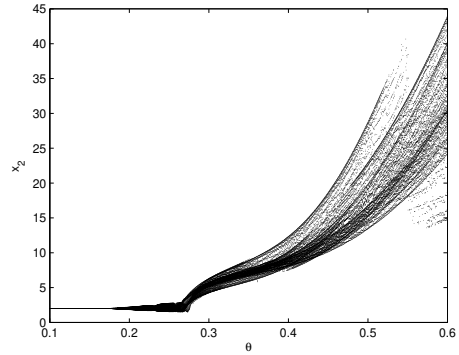

Figure 20. Bifurcation diagram of model (89): the relationship of t and x_2. The bifurcation value of model (89) is about 0.27.

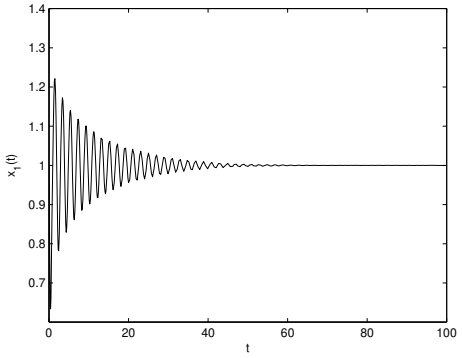

Figure 21. Matlab experiment outcomes of model (90) under the delay $\theta = 0.135 < \theta_\diamond = 0.141$. The positive equilibrium point $E(1, 2)$ keeps locally asymptotically stability. The x-axis represents the time t and the y-axis represents the variable $x_1(t)$.

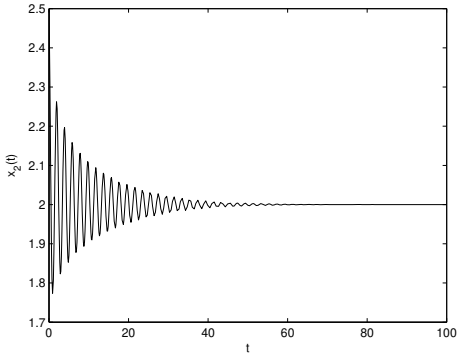

Figure 22. Matlab experiment outcomes of model (90) under the delay $\theta = 0.135 < \theta_\diamond = 0.141$. The positive equilibrium point $E(1, 2)$ keeps locally asymptotically stability. The x-axis represents the time t and the y-axis represents the variable $x_2(t)$.

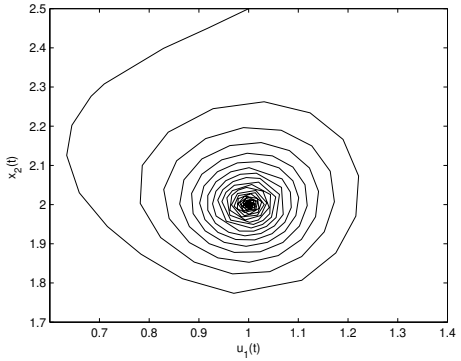

Figure 23. Matlab experiment outcomes of model (90) under the delay $\theta = 0.135 < \theta_\diamond = 0.141$. The positive equilibrium point $E(1, 2)$ keeps locally asymptotically stability. The x-axis represents the time $x_1(t)$ and the y-axis represents the variable $x_2(t)$.

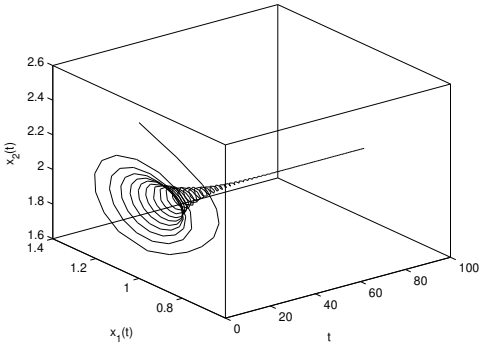

Figure 24. Matlab experiment outcomes of model (90) under the delay $\theta = 0.135 < \theta_\diamond = 0.141$. The positive equilibrium point $E(1, 2)$ keeps locally asymptotically stability. The x-axis represents the time t, the y-axis represents the variable $x_1(t)$ and the z-axis represents the variable $x_2(t)$.

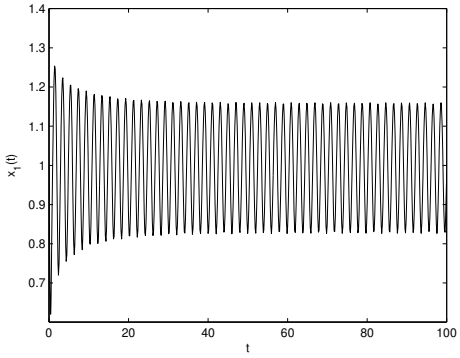

Figure 25. Matlab experiment outcomes of model (90) under the delay $\theta = 0.146 > \theta_\diamond = 0.141$. Hopf bifurcation takes placer around the positive equilibrium point $E(1, 2)$. The x-axis represents the time t and the y-axis represents the variable $x_1(t)$.

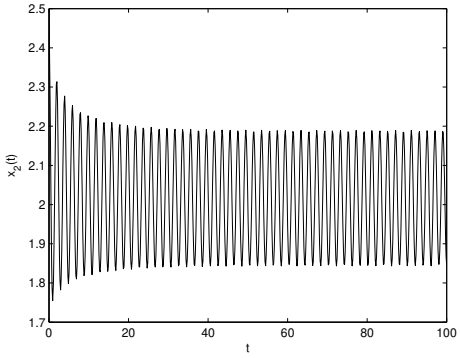

Figure 26. Matlab experiment outcomes of model (90) under the delay $\theta = 0.146 > \theta_\diamond = 0.141$. Hopf bifurcation takes placer around the positive equilibrium point $E(1, 2)$. The x-axis represents the time t and the y-axis represents the variable $x_2(t)$.

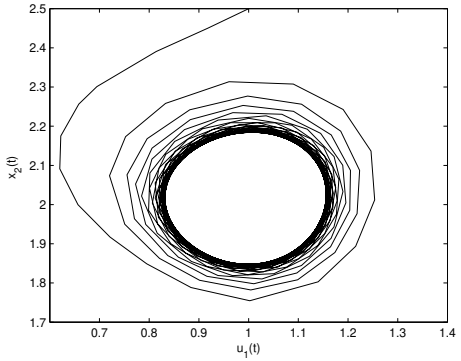

Figure 27. Matlab experiment outcomes of model (90) under the delay $\theta = 0.146 > \theta_\diamond = 0.141$. Hopf bifurcation takes placer around the positive equilibrium point $E(1, 2)$. The x-axis represents the time $x_1(t)$ and the y-axis represents the variable $x_2(t)$.

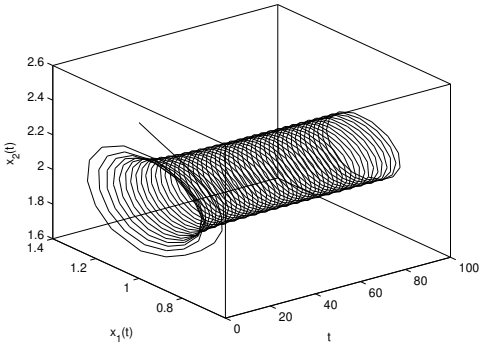

Figure 28. Matlab experiment outcomes of model (90) under the delay $\theta = 0.146 > \theta_\diamond = 0.141$. Hopf bifurcation takes placer around the positive equilibrium point $E(1, 2)$. The x-axis represents the time t, the y-axis represents the variable $x_1(t)$ and the z-axis represents the variable $x_2(t)$.

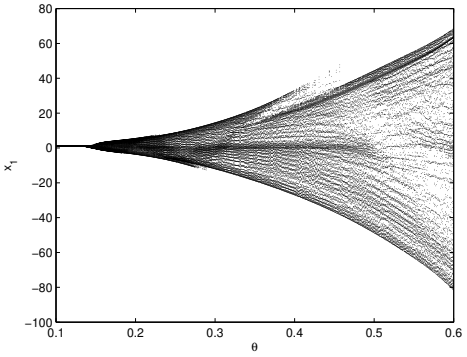

Figure 29. Bifurcation diagram of model (90): the relationship of t and x_1. The bifurcation value of model (90) is about 0.141.

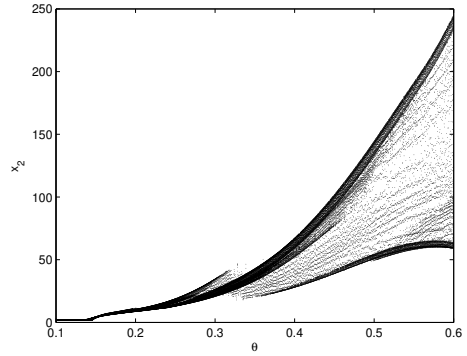

Figure 30. Bifurcation diagram of model (90): the relationship of t and x_2. The bifurcation value of model (90) is about 0.141.

Remark 6.1. *Through numerical simulation outcomes of Example 6.1-Example 6.3, one can enlarge the stability domain and delay the time of generation of Hopf bifurcation of model (88) via nonlinear delayed feedback controller. In addition, one can narrow the stability domain and advance the time of generation of Hopf bifurcation of model (88) via hybrid controller.*

7 Conclusions

Nowadays delayed dynamical models have been widely applied in describing the inherent interaction law among different chemical substances. Relying on the earlier publications, we formulate a new fractional-order delayed Lengyel-Epstein model. Whit the aid of stability and bifurcation theory of fractional-order differential equation, we have explored the stability trait and Hopf bifurcation phenomenon of the addressed fractional-order delayed Lengyel-Epstein model. The sufficient condition on stability and bifurcation for the formulated fractional-order delayed Lengyel-Epstein model are established. By applying two suitable controllers (nonlinear delayed feedback controller and hybrid controller), we have successfully dominated the stability region and the time of Hopf bifurcation periodic solutions for the formulated fractional-order delayed Lengyel-Epstein model. The role of delay in stabilizing Lengyel-Epstein system and adjusting the concentrations of different chemical substances is fully revealed. In order to check the correctness of the gained outcomes, we present the computer simulations. The gained fruits own important significance in controlling and balancing the concentrations of different chemical substances. The exploration way is also able to deal with the control issue in numerous fractional-order dynamical models.

***Acknowledgment*:** This work is supported by National Natural Science Foundation of China (No.12261015, No.62062018), Project of High-level Innovative Talents of Guizhou Province ([2016]5651), Basic research projects of key scientific research projects in Henan province(No.20ZX001), Key Science and Technology Research Project of Henan Province of China (Grant Nos. 222102210053), Key Scientific Research Project in Colleges and Universities of Henan Province of China (Grant Nos.21A510003).

References

[1] A. Din, T. Donchev, D. Kolev, Stability, bifurcation and chaos control in chlorine dioxide-iodine-malonic acid reaction, *MATCH Commun. Math. Comput. Chem.* **79** (2018) 577–606.

[2] Y. Sekerci, S. Petrovskii, Mathematical modelling of plankton-oxygen dynamics under the climate change, *Bull. Math. Biol.* **77** (2015) 2325–2353.

[3] S. Mondal, G. Samanta, Dynamics of a delayed toxin producing plankton model with variable search rate of zooplankton, *Math. Comput. Sim.* **196** (2022) 166–191.

[4] A. Gökçe, S. Yazar, Y. Sekerci, Stability of spatial patterns in a diffusive oxygen-plankton model with time lag effect, *Math. Comput. Sim.* **194** (2022) 109–123.

[5] C. J. Xu, Y. S. Wu, Bifurcation and control of chaos in a chemical system, *Appl. Math. Model.* **39** (2015) 2295–2310.

[6] J. J. Wang, Y. F. Jia, Analysis on bifurcation and stability of a generalized Gray-Scott chemical reaction model, *Phys. A: Stat. Mech. Appl.* **528** (2019) #121394.

[7] T. K. Mankodi, U. V. Bhandarkar, B. P. Puranik, Hypersonic flow over Stardust Re-entry Capsule using ab-initio based chemical reaction model, *Acta Astro.* **162** (2019) 243–255.

[8] D. Kim, M. S. Lee, S. B. Yun, On the positivity of an auxiliary function of the BGK model for slow chemical reactions, *Appl. Math. Lett.* **113** (2021) #106841.

[9] J. Gao, C. G. Gu, H. J. Yang, Spiral waves with interfacial oscillatory chemical reactions emerge in a model of reaction-diffusion systems, *Chem. Phys.* **528** (2020) #110507.

[10] S. P. Clavijo, A. F. Sarmiento, L. F. R. Espath, L. Dalcin, A. M. A. Cortes, V. M. Calo, Reactive n-species Cahn-Hilliard system: A thermodynamically-consistent model for reversible chemical reactions, *J. Comput. Appl. Math.* **350** (2019) 143–154.

[11] Y. H. Zhao, Y. W. Wang, J. P. Shi, Steady states and dynamics of an autocatalytic chemical reaction model with decay, *J. Diff. Eq.* **253** (2012) 533–552.

[12] V. Voorsluijs, Y. D. Decker, Emergence of chaos in a spatially confined reactive system, *Phys. D* **335** (2016) 1–9.

[13] I. Lengyel, I. R. Epstein, Modeling of turing structures in the chlorite-iodide-malonic acid-starch reaction system, *Science* **251** (1991) 650–652.

[14] I. Lengyel, I. R. Epstein, A chemical approach to designing turing patterns in reaction-diffusion systems, *Proc. Nat. Academy Sci.* **89** (1992) 3977–3979.

[15] F. Q. Yi, J. J. Wei, J. P. Shi, Global asymptotical behavior of the lengyel-epstein reaction-diffusion system, *Appl. Math. Lett.* **22** (2009) 52–55.

[16] F. Q. Yi, J. J. Wei, J. P. Shi, Diffusion-driven instability and bifurcation in the Lengyel-Epstein system, *Nonlin. Anal. Real World Appl.* **9** (2008) 1038–1051.

[17] W. M. Ni, M. Tang, Turing patterns in the lengyel-epstein system for the cima reaction, *Trans. Am. Math. Soc.* **357** (2005) 3953–3969.

[18] J. Y. Jin, J. P. Shi, J. J. Wei, Bifurcations of patterned solutions in the diffusive lengyel-epstein system of cima chemical reactions, *Rocky Mountain J. Math.* **43** (2013) 1637–1674.

[19] C. Çelik, H. Merdan, Hopf bifurcation analysis of a system of coupled delayed-differential equations, *Appl. Math. Comput.* **219** (2013) 6605–6617.

[20] H. Merdan, C. Kayan, Hopf bifurcations in lengyel-epstein reaction-diffusion model with discrete time delay, *Nonlin. Dyn.* **79** (2015) 1757–1770.

[21] H. Merdan, C. Kayan, Delay effects on the dynamics of the lengyel-epstein reaction-diffusion model, in: A. C. J. Luo, H. Merdan (Eds.), *Mathematical Modelling and Applications in Nonlinear Dynamics*, Springer, Berlin, 2016, pp. 125-160.

[22] C. H. Zhang, Y. He, Multiple stability switches and hopf bifurcations induced by the delay in a lengyel-epstein chemical reaction system, *Appl. Math. Comput.* **378** (2020) #125201.

[23] L. Li, Y. X. Zhang, Dynamic analysis and Hopf bifurcation of a Lengyel-Epstein system with two delays, *J. Math.* **2021** (2021) #5554562.

[24] K. Udhayakumar, F. A. Rihan, R. Rakkiyappan, J. D. Cao, Fractional-order discontinuous systems with indefinite LKFs: An application to fractional-order neural networks with time delays, *Neur. Netw.* **145** (2022) 319–330.

[25] C. J. Xu, W. Zhang, C. Aouiti, Z. X. Liu, L. Y. Yao, Bifurcation insight for a fractional-order stage-structured predator-prey system incorporating mixed time delays, *Math. Meth. Appl. Sci.* (2023) https://doi.org/10.1002/mma.8981

[26] C. J. Xu, D. Mu, Z. X. Liu, Y. C. Pang, M. X. Liao, C. Aouiti, New insight into bifurcation of fractional-order 4D neural networks incorporating two different time delays, *Commun. Nonlinear Sci. Numer. Simul.* **118** (2023) #107043.

[27] C. J. Xu, Z. X. Liu, P. L. Li, J. L. Yan, L. Y. Yao, Bifurcation mechanism for fractional-order three-triangle multi-delayed neural networks, *Neural Process. Lett.* (2022) `https://doi.org/10.1007/s11063-022-11130-y`.

[28] C. J. Xu, D. Mu, Z. X. Liu, Y. C. Pang, M. X. Liao, P. L. Li, L. Y. Yao, Q. W. Qin, Comparative exploration on bifurcation behavior for integer-order and fractional-order delayed BAM neural networks, *Nonlin. Anal. Model. Control* **27** (2022) 1030–1053.

[29] C. D. Huang, H. Liu, X. P. Chen, M. S. Zhang, L. Ding, J. D. Cao, A. Alsaedi, Dynamic optimal control of enhancing feedback treatment for a delayed fractional order predator-prey model, *Phys. A* **554** (2020) #124136.

[30] M. Xiao, W. X. Zheng, G. P. Jiang, J. D. Cao, Qualitative analysis and bifurcation in a nneuron system with memristor characteristics and time delay, *IEEE Trans. Neural Netw. Learn. Syst.* **32** (2021) 1974–1988.

[31] M. Xiao, W. X. Zheng, G. P. Jiang, Bifurcation and oscillatory dynamics of delayed cyclic gene networks includingsmall RNAs, *IEEE Trans. Cyber.* **49** (2019) 883–896.

[32] Y. T. Lin, J. L. Wang, C. G. Liu, Output synchronization analysis and PD control for coupled fractional-order neural networks with multiple weights, *Neurocomputing* **519** (2023) 17–25.

[33] C. A. Popa, Mittag-Leffler stability and synchronization of neutral-type fractional-order neural networks with leakage delay and mixed delays, *J. Franklin Inst.* **360** (2023) 327–355.

[34] F. B. Yousef, A. Yousef, C. Maji, Effects of fear in a fractional-order predator-prey system with predator density-dependent prey mortality, *Chaos Solitons Fractals* **145** (2021) #110711.

[35] F. A. Rihan, C Rajivganthi, Dynamics of fractional-order delay differential model of prey-predator system with Holling-type III and infection among predators, *Chaos Solitons Fractals* **141** (2020) #110365.

[36] S. Djilali, B. Ghanbari, S. Bentout, A. Mezouaghi, Turing-Hopf bifurcation in a diffusive mussel-algae model with time-fractional-order derivative, *Chaos Solitons Fractals* **138** (2020) #109954.

[37] J. Alidousti, Stability and bifurcation analysis for a fractional prey-predator scavenger model, *Appl. Math. Model.* **81** (2020) 342–355.

[38] C. J. Xu, Z. X. Liu, Y. C. Pang, A. Akgül, D. Baleanu, Dynamics of HIV-TB coinfection model using classical and Caputo piecewise operator: A dynamic approach with real data from South-East Asia, European and American regions, *Chaos Solitons Fractals* **165** (2022) #112879.

[39] C. J. Xu, M. Rahman, D. Baleanu, On fractional-order symmetric oscillator with offset-boosting control, *Nonlin. Anal. Model. Control* **27** (2022) 994–1008.

[40] C. J. Xu, M. X. Liao, P. L. Li, L. Y. Yao, Q. W. Qin, Y. L. Shang, Chaos control for a fractional-order Jerk system via time delay feedback controller and mixed controller, *Fract. Fractional* **5** (2021) #257.

[41] I. Podlubny, *Fractional Differential Equations*, Academic Press, New York, 1999.

[42] D. Matignon, Stability results for fractional differential equations with applications to control processing, in: *Computational Engineering in Systems and Application Multi-Conference, IMACS, IEEE-SMC Proceedings*, Lille, 1996, pp. 963–968.

[43] H. L. Li, L. Zhang, C. Hu, Y. L. Jiang, Z. D. Teng, Dynamical analysis of a fractional-order predator-prey model incorporating a prey refuge, *J. Appl. Math. Comput.* **54** (2017) 435–449.

[44] Q. S. Sun, M. Xiao, B.B. Tao, Local bifurcation analysis of a fractional-order dynamic model of genetic regulatory networks with delays, *Neur. Process. Lett.* **47** (2018) 1285–1296.

[45] P. Yu, G. R. Chen, Hopf bifurcation control using nonlinear feedback with polynomial functions, *Int. J. Bifur. Chaos* **14** (2004) 1683–1704.

[46] Z. Z. Zhang, H. Z. Yang, Hybrid control of Hopf bifurcation in a two prey one predator system with time delay, in: *Proceeding of the 33rd Chinese Control Conference*, Nanjing, 2014, pp. 6895–6900.

[47] L. P. Zhang, H. N. Wang, M. Xu, Hybrid control of bifurcation in a predator-prey system with three delays, *Acta Phys. Sinica* **60** (2011) #010506.